IOPscience iopscience.iop.org

Home Search Collections Journals About Contact us My IOPscience

Absolute-convective instability of mixed forced-free convection boundary layers

This content has been downloaded from IOPscience. Please scroll down to see the full text.

2010 Fluid Dyn. Res. 42 055506

(http://iopscience.iop.org/1873-7005/42/5/055506)

View the table of contents for this issue, or go to the journal homepage for more

Download details:

IP Address: 196.44.162.122
This content was downloaded on 07/03/2014 at 15:24

Please note that terms and conditions apply.

IOP PUBLISHING FLUID DYNAMICS RESEARCH

Fluid Dyn. Res. **42** (2010) 055506 (10pp) doi:10.1088/0169-5983/42/5/055506

Absolute-convective instability of mixed forced-free convection boundary layers

Eunice W Mureithi[1] **and James P Denier**[2]

[1] Department of Mathematics and Applied Mathematics, University of Pretoria, Pretoria 0002, South Africa
[2] School of Mathematical Sciences, University of Adelaide, South Australia 5005, Australia

E-mail: eunice.mureithi@up.ac.za

Received 1 December 2009, in final form 19 July 2010
Published 18 August 2010
Online at stacks.iop.org/FDR/42/055506

Communicated by A D Gilbert

Abstract

A spatio-temporal inviscid instability of a mixed forced-free convection boundary layer is investigated. The base flow considered is the self-similar flow with free-stream velocity $u_e \sim x^n$. Such a boundary-layer flow presents the unusual behaviour of generating a region of velocity overshoot, in which the streamwise velocity within the boundary layer exceeds the free-stream speed. A linear stability analysis has been carried out. Saddle points have been located and a critical value for the buoyancy parameter, $G_{0c} \approx 3.6896$, has been determined below which the flow is convectively unstable and above which the flow becomes absolutely unstable. Two spatial modes have been obtained, one mode being convective in nature and the other absolute. The convective-type spatial mode shows mode crossing behaviour at lower frequencies. Thermal buoyancy is shown to be destabilizing to the absolutely unstable spatial mode.

1. Introduction

The linear spatio-temporal stability analysis has become an important tool for investigating the initial stages of transition to turbulence. The properties of linear stability of boundary-layer flows are determined from the dispersion relation

$$D(\alpha, \Omega; \mathbf{R}) = 0,$$

where α and Ω are the wavenumber and the wave frequency, respectively. $\mathbf{R}$ represents the parameters of the problem. Traditionally, two approaches are used to determine the linear stability, namely a temporal stability analysis in which α is real and Ω is complex and a spatial stability analysis in which α is complex and Ω is real. The temporal approach is satisfactory for closed flows such as Taylor–Couette flow but is inadequate for open flows, such as flow

© 2010 The Japan Society of Fluid Mechanics and IOP Publishing Ltd Printed in the UK
0169-5983/10/055506+10$30.00

past a flat plate where spatial growth/decay may occur. For a more complete analysis for open flows, the spatio-temporal analysis where both α and Ω are complex valued is necessary.

A parallel flow is absolutely unstable if localized disturbances grow exponentially, eventually contaminating the entire flow. A flow is convectively unstable if disturbances are convected from the source (see Huerre and Monkewitz 1990).

Extensive studies on absolute/convective instability of rotating disc boundary-layer flows have been conducted by, among others, Lingwood (1995) and Turkyilmazoglu *et al* (2000). A comprehensive review on absolute/convective instability of shear layers is given by Huerre and Monkewitz (1985). Investigations on absolute and convective instabilities in mixed convection boundary layers have been reported for flows over isothermal vertical walls by, among others, Krizhevsky *et al* (1996) and Moresco and Healey (2000) where they showed that reverse flow regions are more prone to absolute instability.

The current study aims to explore absolute/convective instability in mixed forced-free convection boundary-layer flow over a horizontal surface. This study has been prompted by results obtained in temporal stability studies of mixed forced-free convection boundary layers by Denier and Mureithi (1996), Denier *et al* (1997), Mureithi *et al* (1997) and Mureithi and Mason (2002). Such boundary layers were found to be characterized by internal regions of 'supervelocities' due to acceleration of the boundary-layer flow by a buoyancy-induced pressure gradient.

In section 2, the governing equations for the flow and the boundary-layer equations are formulated. In section 3, the linearized spatial stability equations are presented. Formulation of the absolute-convective stability is presented in section 4. Discussion of our results is given in section 5 and conclusions are drawn in section 6.

2. Formulation of the problem

A two-dimensional flow of a viscous incompressible fluid, of density ρ and kinematic viscosity ν, over a heated flat plate is considered. The equations governing the motion of the fluid in non-dimensional form and under the Boussinesq approximation are

$$\nabla \cdot \mathbf{q} = 0,$$
$$\left(\frac{\partial}{\partial t} + \mathbf{q}\cdot\nabla\right)\mathbf{q} = -\nabla p + \frac{1}{Re}\nabla^2\mathbf{q} + \mathbf{b}T - \mathbf{c},$$
$$\left(\frac{\partial}{\partial t} + \mathbf{q}\cdot\nabla\right)T = \frac{1}{Pr\ Re}\nabla^2 T,$$

where $T(x, y, t)$ is the temperature distribution function and

$$\mathbf{q}^{\mathrm{T}} = (u,\ v), \quad \mathbf{b}^{\mathrm{T}} = (0,\ G), \quad \mathbf{c}^{\mathrm{T}} = \left(0,\ \frac{gL}{U_\infty^2}[1 + \beta(T_0 - T_\infty)]\right)$$

with the superscript 'T' representing the transpose. Here Pr is the Prandtl number, $G = GrRe^{-2}$ is the buoyancy parameter introduced by Denier and Mureithi (1996) with $Gr = g\beta L^3(T_0 - T_\infty)/\nu^2$ being the Grashof number, β the coefficient of volume expansion, ν the kinematic viscosity and g the acceleration due to gravity. All velocities have been non-dimensionalized by the free-stream speed U_∞, distances by a typical length-scale L (for example, distance measured from the leading edge of the plate), pressure by $\rho_0 U_\infty^2$, time by L/U_∞ and temperature by $(T_0 - T_\infty)$, where T_∞ is the free-stream temperature and T_0 is the temperature of the plate. Here ρ_0 is the density at temperature T_0 and the Reynolds number Re is defined as $Re = U_\infty L/\nu$.

2.1. Boundary-layer equations

In the limit of a large Reynolds number the flow develops a boundary layer of thickness $O(Re^{-1/2})$ attached to the leading edge of the plate. The boundary-layer scalings are

$$y = Re^{-1/2}Y, \quad (u(x, y), v(x, y), T(x, y)) = (\bar{u}(x, Y), Re^{-1/2}\bar{v}(x, Y), \bar{T}),$$

$$p(x, y) - \tilde{P}(y) = -\tfrac{1}{2}u_e^2 + G\, Re^{-1/2}\, \bar{p}(x, Y),$$

where $u_e(x)$ is the scaled free-stream speed, $\bar{p}(x, Y)$ is the buoyancy-induced pressure term and $\tilde{P}(y)$ is the hydrostatic pressure satisfying the equation

$$\frac{\mathrm{d}\tilde{P}}{\mathrm{d}y} = -\frac{gL}{U_\infty^2}[1 + \beta(T_0 - T_\infty)].$$

This hydrostatic pressure gradient balances the gravitational force. The pressure component $-\frac{1}{2}u_e^2(x)$ has been introduced to accommodate a possible non-uniform streaming velocity $u_e(x)$ in the far field.

Substituting these scalings in the governing equations and taking the formal limit $Re \to \infty$, we have the coupled boundary-layer equations

$$\left.\begin{aligned} &\frac{\partial \bar{u}}{\partial x} + \frac{\partial \bar{v}}{\partial y} = 0, \\ &\bar{u}\frac{\partial \bar{u}}{\partial x} + \bar{v}\frac{\partial \bar{u}}{\partial Y} = u_e(x)\frac{\mathrm{d}u_e}{\mathrm{d}x} - G\, Re^{-1/2}\frac{\partial \bar{p}}{\partial x} + \frac{\partial^2 \bar{u}}{\partial Y^2}, \\ &\frac{\partial \bar{p}}{\partial Y} = \bar{T}, \\ &\bar{u}\frac{\partial \bar{T}}{\partial x} + \bar{v}\frac{\partial \bar{T}}{\partial Y} = \frac{1}{Pr}\frac{\partial^2 \bar{T}}{\partial Y^2}, \end{aligned}\right\} \tag{2.1}$$

with boundary conditions

$$\left.\begin{aligned} &\bar{u} = \bar{v} = \bar{T} - T_e(x) = 0, \qquad \text{at} \qquad Y = 0, \\ &\bar{u} \to u_e(x), \quad \bar{T} \to 0, \qquad \text{as} \qquad Y \to \infty. \end{aligned}\right\} \tag{2.2}$$

If the buoyancy parameter is scaled such that buoyancy has an $O(1)$ effect on the leading-order boundary-layer flow, then we require $G = Re^{1/2}G_0$ with $G_0 = O(1)$. It is instructive to note the effect of the buoyancy parameter G_0 on the basic flow. In the limit $G_0 \to 0$, the buoyancy-induced horizontal pressure gradient appearing in the second equation in (2.1) vanishes, the energy and momentum fields decouple and the governing equations reduce to those for the usual *forced* convection boundary layer in which the temperature of the basic flow is essentially passive. Conversely as $G_0 \to \infty$ equations (2.1) must be rescaled as $(\bar{u}, \bar{v}, \bar{p}, \bar{T}) = (G_0^{2/5}\bar{u}_0, G_0^{1/5}\bar{v}_0, G_0^{-1/5}\bar{p}, \bar{T}_0)$ with the new boundary-layer variable given by $z = G_0^{1/5}Y$, and in this new limit the flow is governed by the free-convection boundary-layer equations. In the current study attention is restricted to the intermediate regime $G_0 = O(1)$—such flows are commonly referred to as *mixed forced-free* convection boundary layers.

Equations (2.1) admit a family of self-similar solutions given by

$$\bar{u} = x^n f'(\eta), \quad \bar{T} = x^{(5n-1)/2}\theta(\eta), \quad \bar{p} = x^{2n}q(\eta),$$

where the similarity variable is $\eta = Yx^{(n-1)/2}$ and the far-field is taken to be $u_e = x^n$. Under this transformation, system (2.1) reduces to

$$\left.\begin{aligned} f''' &= n\left(f'^2 - 1\right) - \tfrac{1}{2}(n+1)ff'' + 2nqG_0 + \tfrac{1}{2}(n-1)G_0\eta q', \\ q' &= \theta, \\ \theta'' &= \frac{Pr}{2}[(5n-1)\theta f' - (n+1)f\theta'], \end{aligned}\right\} \tag{2.3}$$

subject to the boundary conditions

$$f(0) = f'(0) = 0, \quad \theta(0) = 1, \quad f'(\infty) = 1, \quad q(\infty) = \theta(\infty) = 0. \tag{2.4}$$

The boundary-layer equations describe the self-similar flow over a wedge making an angle $n\pi/(n+1)$. We note that the only choice of similarity variable which allows for the plate temperature to remain constant is for $n = 1/5$. For the sake of definiteness we will focus on this case and make some comments regarding the behaviour of the flow for other values of n.

The two-point boundary value problem described by (2.3) with boundary conditions (2.4) was solved by using a standard shooting technique which employed a fourth-order Runge–Kutta quadrature scheme as the integrator.

An important characteristic of this buoyant boundary-layer flow is that it can develop supervelocities, where the streamwise velocity acquires a velocity that exceeds the free-stream value of unity, inside the boundary layer. Some typical results are shown in figures 1(a) and 2, where we note that there is a finite region within the boundary layer where the streamwise velocity overshoots its free-stream value. An in-depth analysis of this type of basic flow has been presented by Denier and Mureithi (1996). Thermal buoyancy, through the pressure term $\bar{p}(x, Y)$, induces an additional streamwise pressure gradient in the horizontal momentum equation. Far enough from the heated surface the decelerating effect of the skin friction is outbalanced by the increased acceleration, thus giving rise to supervelocities within the boundary layer.

3. Spatial instability

Upon the basic boundary-layer flow (2.1) we superimpose inviscid disturbances proportional to $\exp[Re^{1/2}(\mathrm{i}\alpha x - \mathrm{i}\Omega t)]$, where Ω is a real prescribed frequency and $\alpha = \alpha_\mathrm{r} + \mathrm{i}\alpha_\mathrm{i}$ is the complex 'wavenumber' that is to be determined. The equations governing the disturbance amplitude can be placed in the form of the classical Taylor–Goldstein equation

$$\left(\bar{u} - \frac{\Omega}{\alpha}\right)^2 \left(\frac{\partial^2}{\partial Y^2} - \alpha^2\right) V - \left[\left(\bar{u} - \frac{\Omega}{\alpha}\right)\bar{u}_{YY} - G_0\bar{T}_y\right] V = 0. \tag{3.1}$$

This equation, when supplemented by boundary conditions

$$V = 0 \quad \text{on} \quad Y = 0, \qquad V \quad \text{bounded as} \quad Y \to \infty,$$

defines an eigenvalue problem for the complex eigenfunction V and the complex 'wavenumber' α as a function of the frequency Ω. A downstream propagating mode is deemed unstable if $\mathrm{Im}(\alpha) < 0$ and vice versa for an upstream propagating mode.

Equation (3.1) was solved by first replacing the homogeneous boundary condition $V = 0$ on $Y = 0$ by the inhomogeneous normalization condition $V_Y = 1$ on $Y = 0$. The resulting

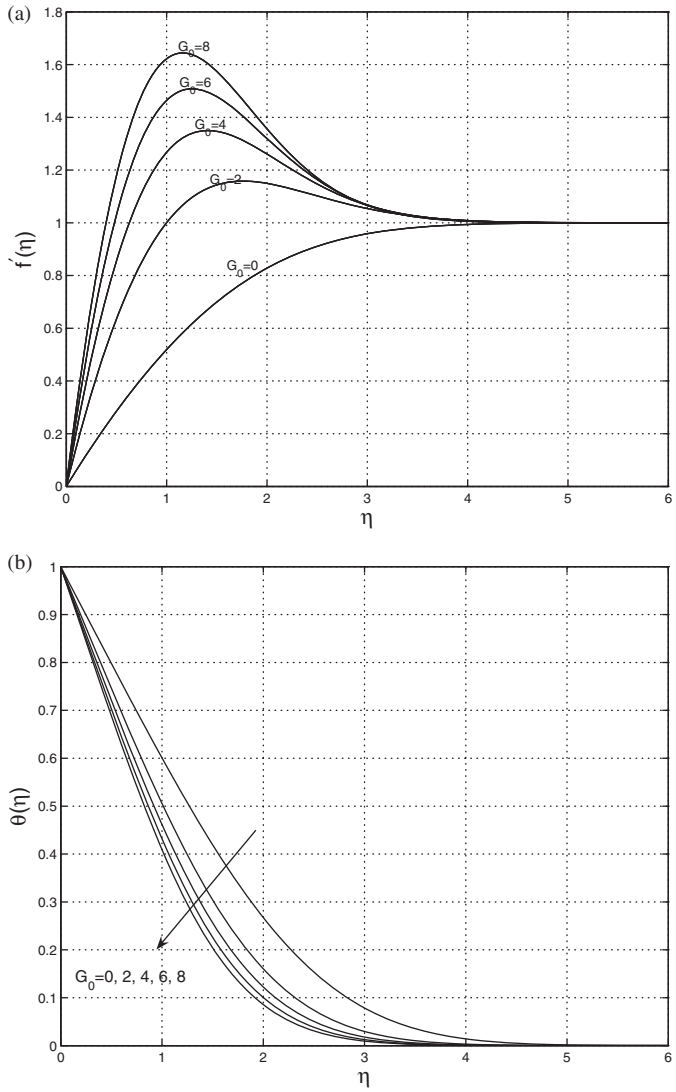


Figure 1. Plot of the similarity solutions (a) $f'(\eta)$ and (b) $\theta(\eta)$ for various G_0 values and for $n = 1/5$.

equation was then discretized using second-order accurate centred differences. The boundary conditions were satisfied explicitly, with the far-field boundary condition being replaced by the Robin-type boundary condition

$$\frac{1}{V}\frac{\partial V}{\partial Y} = -\alpha, \qquad Y \to \infty.$$

Newton iteration was then used to determine the complex value of α at which the remaining boundary condition $V = 0$ on $Y = 0$ was satisfied.

The results are presented in figures 3 and 4. Figure 3 shows the presence of two spatial modes in the complex α-plane, one defined for $G_0 < 3.7$ and the other for $G_0 \geqslant 3.7$. Figures 4(a) and (b) show the real and the imaginary parts of α as functions of Ω at various values of G_0. These results again show a distinction between the two spatial modes. The

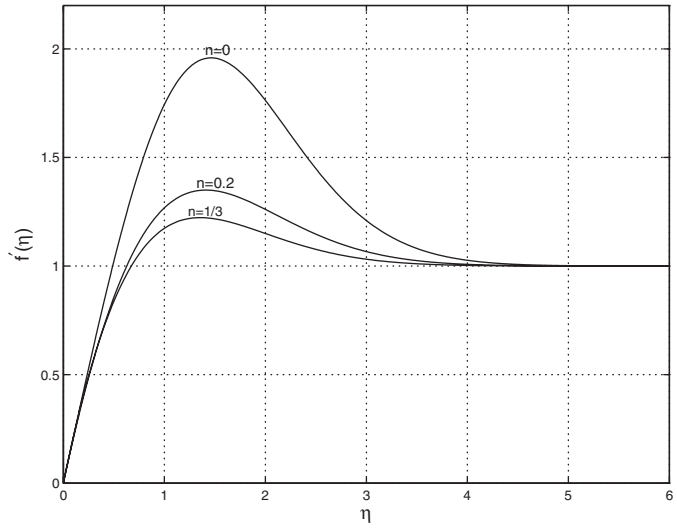


Figure 2. $f'(\eta)$ versus η for $G_0 = 4$ and for $n = 0,\ 0.2,\ 1/3$.

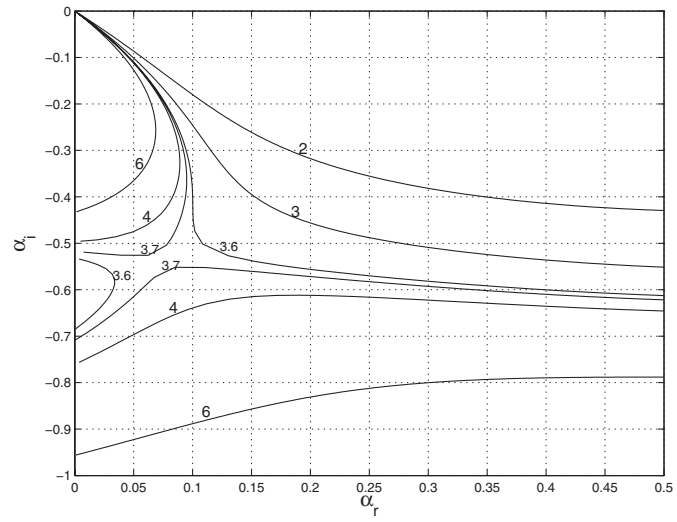


Figure 3. Plot of $\alpha_{\rm i}$ (the imaginary part of α) versus $\alpha_{\rm r}$ (the real part of α) for various values of G_0. Two spatial families are shown here.

findings suggest the necessity to look into the absolute/convective instability of the flow in an effort to distinguish these modes of instability.

4. Absolute versus convective instability

In this case, both α and Ω in the dispersion relation $D(\alpha, \Omega; G_0) = 0$ are complex valued.

To determine the absolute/convective nature of instability, the Taylor–Goldstein equation (3.1) was solved using a shooting technique for complex $\alpha = \alpha_{\rm r} + {\rm i}\alpha_{\rm i}$ and complex $\Omega = \Omega_{\rm r} + {\rm i}\Omega_{\rm i}$. The saddle points were located by solving for simultaneous zeros of the

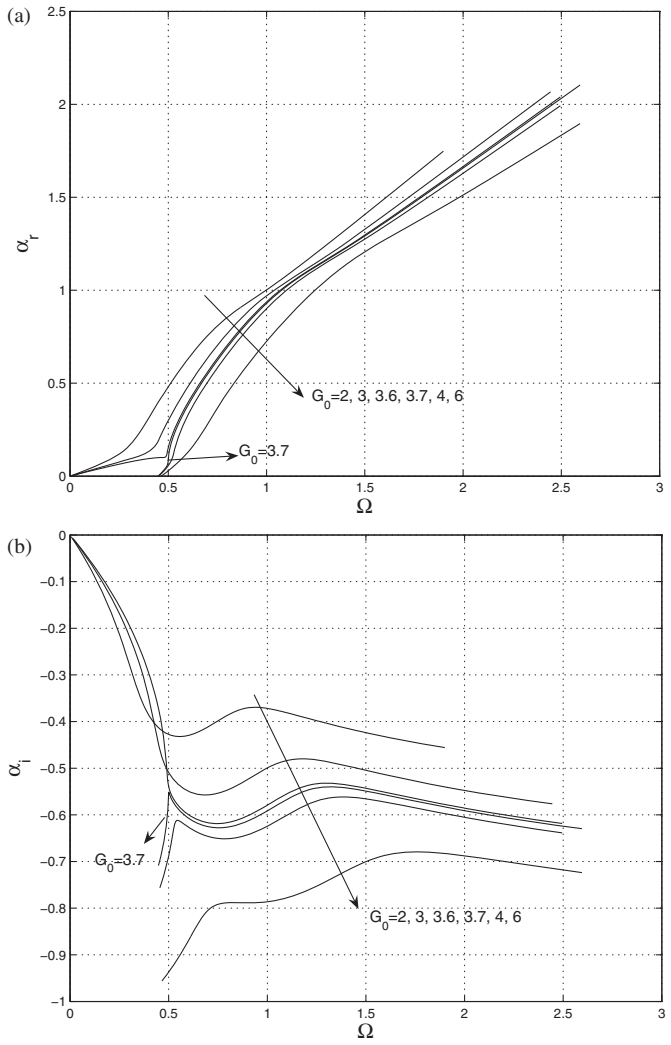


Figure 4. (a) The real and (b) the imaginary parts of α versus Ω for $G_0 = 2, 3, 3.6, 3.7, 4, 6$. For $G_0 < 3.7$ mode crossing is observed when $\Omega < 0.5$.

dispersion relation and the complex group velocity, that is,

$$D(\alpha, \Omega, G_0) = 0, \quad \frac{\partial \Omega}{\partial \alpha} = 0$$

with Pr fixed. The saddle points $\Omega^0(\alpha^0)$ of the dispersion relation in the complex α-plane were determined using an iterative method described by Yin *et al* (2000). According to the Briggs–Bers criterion (Briggs 1964, Bers 1975), a flow is absolutely unstable if $\mathrm{Im}(\Omega) > 0$ and two spatial branches, $\alpha^+(\Omega)$ and $\alpha^-(\Omega)$, originating from distinct halves of the α-plane, have a pinch-point occurring either in the lower or in the upper half of the plane. If $\mathrm{Im}(\Omega) < 0$ at a pinch-point, the flow is convectively unstable. At a saddle point α^0 and Ω^0 are referred to as the absolute wavenumber and absolute wave frequency, respectively.

Table 1. Saddle points corresponding to various values of the buoyancy parameter, G_0.

G_0	Ω_r^0	Ω_i^0	α_r^0	α_i^0
3.0	0.440 079 93	−0.030 352 823	0.050 200 291	−0.520 983 52
3.5	0.482 721 43	−0.007 702 030 6	0.067 388 877	−0.533 382 00
3.6896	0.498 951 34	$0.135\,594\,66 \times 10^{-5}$	0.073 347 948	−0.538 287 52
4.0	0.528 019 29	0.010 354 372	0.082 874 924	−0.547 933 52
6.0	0.673 178 76	0.082 763 252	0.127 046 48	−0.586 663 96
8.0	0.795 032 16	0.146 776 31	0.157 546 92	−0.615 258 22

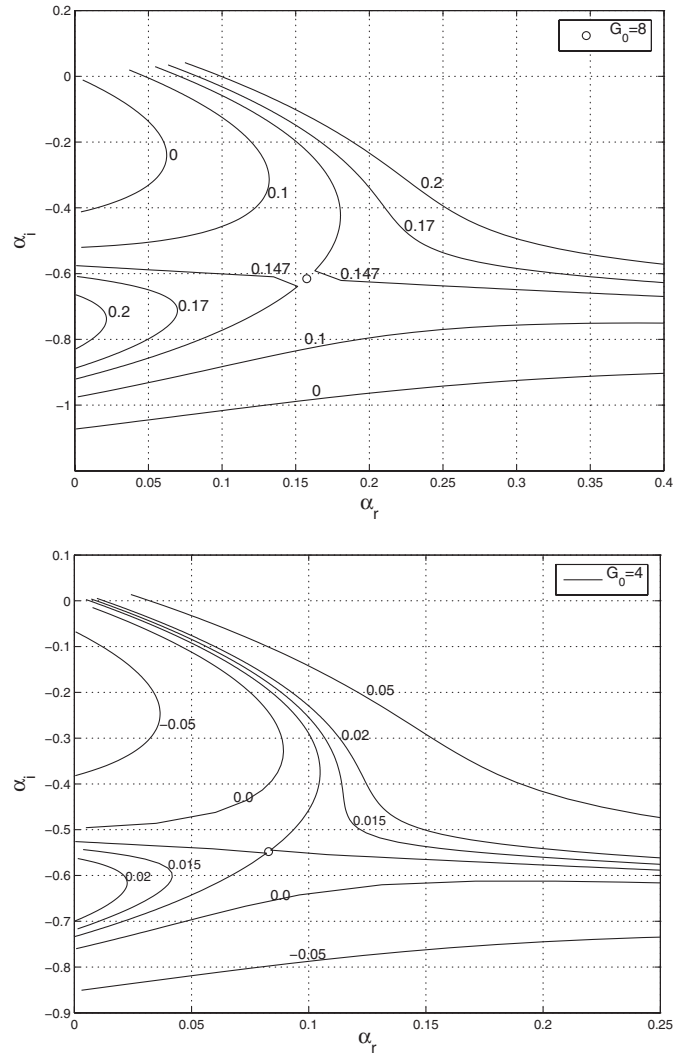


Figure 5. Level curves $\Omega_i = \text{constant}$ in the α-plane. Shown are saddle points for $G_0 = 4$ and $G_0 = 8$. The calculated results show that $(\Omega^0, \alpha^0) = ((0.528\,019\,29, 0.010\,354\,372), (0.082\,874\,924, -0.547\,933\,52))$ for $G_0 = 4$ and $(\Omega^0, \alpha^0) = ((0.795\,032\,16, 0.146\,776\,30), (0.157\,548\,83, -0.615\,259\,47))$ for $G_0 = 8$.

The locations of the saddle points are given in table 1 and presented graphically in figure 5 for two representative cases of G_0.

5. Results and discussion

The self-similar basic flow solutions are presented in figures 1 and 2 for the case when $Pr = 1$. The velocity overshoot behaviour is shown to increase with increasing G_0. This is due to acceleration of the boundary-layer flow by the buoyancy-induced pressure gradient. Increasing n, the pressure gradient parameter, results in decrease in the magnitude of the overshoot, for a fixed G_0. Buoyancy effects are more dominant in flows with no free-stream pressure gradient. The velocity overshoot causes the flow to have points of inflexion, thus rendering the basic flow susceptible to inviscidly unstable short wavelength disturbances as has been detailed by Denier *et al* (1997).

Figure 3 shows two spatial modes in the complex α-plane, each mode having a pair of branches for a fixed value of G_0. For convenience, we will refer to these modes as mode 1 (defined for $G_0 < 3.7$) and mode 2 (defined for $G_0 \geqslant 3.7$). Mode 2 becomes more unstable as G_0 increases. The upstream branch of mode 2 is defined at very small wavenumber values ($\alpha_r < 0.1$). Presented in figure 4 is a plot of the real and imaginary parts of α as functions of the real frequency Ω for various values of G_0. The figure confirms the presence of the two distinct spatial modes, for the cases when $G_0 < 3.7$ and $G_0 \geqslant 3.7$, respectively. Mode 1 shows evidence of mode crossing and stabilization when $\Omega < 0.5$. Mode 2 becomes more spatially unstable as G_0 increases.

Table 1 shows the locations of saddle points corresponding to various values of G_0. Our results indicate that there exists a critical value of G_0, given as $G_{0c} \approx 3.6896$, for $n = 0.5$ and $Pr = 1$, that marks the transition from one spatial mode of instability to another. In figure 5 spatial branches, $\alpha^-(\Omega_r)$ and $\alpha^+(\Omega_r)$, are shown at various fixed values of Ω_i. Also presented in figure 5 are some typical pinch-points in the lower half of the α-plane for the cases when $G_0 = 4$ and $G_0 = 8$. At the pinch-points $\mathrm{Im}(\Omega) > 0$. From these results, we can ascertain that spatial mode 2 (for $G_0 > G_{0c}$) is absolute in nature and mode 1 ($G_0 < G_{0c}$) is convective. These results also show that the absolutely unstable mode is destabilized by thermal buoyancy.

6. Conclusion

Linear stability analysis has been used to examine the role of thermal buoyancy on the transition from convective to absolute instability in a mixed forced-free convection boundary layer. From the absolute/convective analysis, a critical value $G_{0c} \approx 3.6896$, for the case when $Pr = 1$ and $n = 0.2$, has been determined below which the flow is convectively unstable and above which absolute instability sets in. The spatial stability results show two spatial modes, one of which is destabilized by thermal buoyancy. The two modes have been shown to be either absolutely unstable ($G_0 > G_{0c}$) or convectively unstable ($G_0 < G_{0c}$). The absolute instability increases with increase in thermal buoyancy. The convective spatial mode ($G_0 < G_{0c}$) has been shown to be characterized by very small wavenumbers ($\alpha_r < 0.1$) and by mode crossing behaviour at lower frequencies ($\Omega < 0.5$).

Acknowledgments

This work was supported by the National Research Foundation, Pretoria, South Africa, under grant number 2053745 and the University of Pretoria Research Development Programme.

References

Bers A 1975 Linear waves and instabilities *Plasma Physics* ed C DeWitt and J Peyraud (New York: Gordon and Breach)

Briggs R J 1964 *Electron-Stream Interaction with Plasma* (Research monograph no 29) (Cambridge, MA: MIT Press)

Huerre P and Monkewitz P A 1985 Absolute and convective instabilities in free shear layers *J. Fluid Mech.* **159** 151–68

Huerre P and Monkewitz P A 1990 Local and global instabilities in spatially developing flows *Annu. Rev. Fluid Mech.* **22** 473–537

Denier J P and Mureithi E W 1996 Weakly nonlinear wave motions in a thermally stratified stratified boundary layers *J. Fluid Mech.* **315** 293–316

Denier J P, Mureithi E W and Stott J A K 1997 Nonlinear wave motions in stratified boundary layers *Theor. Comput. Fluid Dyn.* **10** 105–14

Krizhevsky L, Cohen J and Tanny J 1996 Convective and absolute instabilities of a buoyancy induced flow in a thermally stratified medium *Phys. Fluids* **8** 971–7

Lingwood R J 1995 Absolute instability of a boundary layer on a rotating disk *J. Fluid Mech.* **299** 17–33

Moresco P and Healey J J 2000 Spatio-temporal stability in mixed convection boundary layers *J. Fluid Mech.* **402** 89–107

Mureithi E W, Denier J P and Stott J A K 1997 The effect of buoyancy on upper branch Tollmien–Schlichting waves *IMA J. Appl. Math.* **58** 19–50

Mureithi E W and Mason D P 2002 The effect of viscous dissipation on the stability of buoyant boundary layer *Fluid Dyn. Res.* **31** 65–78

Turkyilmazoglu M, Cole J W and Gajjar J S B 2000 Absolute and convective instabilities in the compressible boundary layer on a rotating disk *Theor. Comput. Fluid Dyn.* **14** 21–37

Yin X, Sun D and Wei M 2000 Absolute and convective instability character of slender viscous vortices *Phys. Fluids* **12** 1062–72